This is to certify that the

thesis entitled

The Relationship Between Particle Size and Deformation Induced-Martensitic Transformation of Iron Particles in Cu-1%Fe Single Crystals

presented by

Can Mehmet Toksoy

has been accepted towards fulfillment
of the requirements for

M.S. degree in Materials Science

George E. Mase,
Acting Chairman
for.
M. Kato

Major professor

Date Aug. 12, 1982

THE RELATIONSHIP BETWEEN PARTICLE SIZE AND DEFORMATION INDUCED MARTENSITIC TRANSFORMATION OF IRON PARTICLES IN Cu-1%Fe SINGLE CRYSTALS

By

CAN MEHMET TOKSOY

A THESIS

Submitted to
Michigan State University
in partial fulfillment of the requirements
for the degree of

MASTER OF SCIENCE

Department of Metallurgy, Mechanics
and Material Science

1982

ABSTRACT

THE RELATIONSHIP BETWEEN PARTICLE SIZE AND DEFORMATION-INDUCED MARTENSITIC TRANSFORMATION OF IRON PARTICLES IN Cu-1%Fe SINGLE CRYSTALS

By

CAN MEHMET TOKSOY

The small (150 to 1400 Å diameter) γ-iron particles in a copper matrix can be transformed to α-iron martensitically if external stress is applied. In this study, single crystals of Cu-1%Fe with spherical γ-iron particles were deformed in tension along the [100] direction to induce $\gamma \rightarrow \alpha$ martensitic transformation. The particle size was observed as a function of time by utilizing transmission electron microscopy. As a supplement to the TEM studies, a superconducting susceptometer (SQUID) was used to measure the magnetization of the specimens containing γ and/or α particles at 250 K. These studies are aimed at understanding the relationship between the particle size, amount of deformation and transformation.

ACKNOWLEDGEMENTS

The author would like to express his deepest appreciation to his major advisor Dr. Masaharu Kato for his encouraging advice and guidance in both areas of experimental study and writing this thesis. Thanks are also due to Dr. K. Mukherjee for his helpfull discussion, to Dr. W. Pratt for his kind assistance on susceptibility measurements and to Mrs. J. S. Pak for her co-operation on TEM observations. This research is partially supported by the Division of Engineering Research Grant and by the All University Research Initiation Grant at Michigan State University.

TABLE OF CONTENTS

LIST OF FIGURES

1 INTRODUCTION

It is known that in a bulk iron, f.c.c. austenite (γ-iron) transforms in b.c.c. ferrite (α-iron) at a temperature around 1183 K and thus, the stable room-temperature phase of iron is the α-phase. If small spherical iron particles are dispersed in a copper matrix, the γ-iron can stay metastable even below room temperature. This stabilization of the γ-iron is believed to be due to the strong constraint of the f.c.c. copper matrix and consequently, there exists a one-to-one correspondence (usually called "coherency") between the surrounding copper and the γ-iron atoms. These metastable γ-iron particles can transform into the stable α-iron with a martensitic reaction if the specimen is deformed by external stress.

Although many investigators have examined the crystallography and mechanical/physical properties associated with the transformation, it seems that the exact mechanism as to when and how the transformation is initiated is not clearly understood. As a matter of fact, this question is now one of the most important questions in the research area of martensitic transformations.

1.1 Prior Art on the Cu-Fe System

The studies on the Cu-Fe alloys started at 1939 when Bitter and Kauffman[1] suggested that the coherent and spherical γ-iron precipitates in copper matrix transform to b.c.c. α-iron when the alloy was cold worked. In 1940's Smith discovered that paramagnetic γ-iron precipitates in the Cu-2.5wt%Fe alloy transform instantly to the ferromagnetic α-iron following the cold working and this transformation was thought to be martensitic[2].

Figure 1 shows the equilibrium phase diagram of the Cu-Fe system. The maximum solubility of iron in copper is 4wt% at 1356 K and decreases to practically zero at room temperature. If the solution treated Cu-Fe alloy with less than 4wt% iron is aged, say at 973 K, homogeneous nucleation leads to the precipitation of fully coherent, spherical iron particles. Although the phase diagram suggests that the b.c.c. α-iron should be the equilibrium phase at 973 K, the precipitated iron

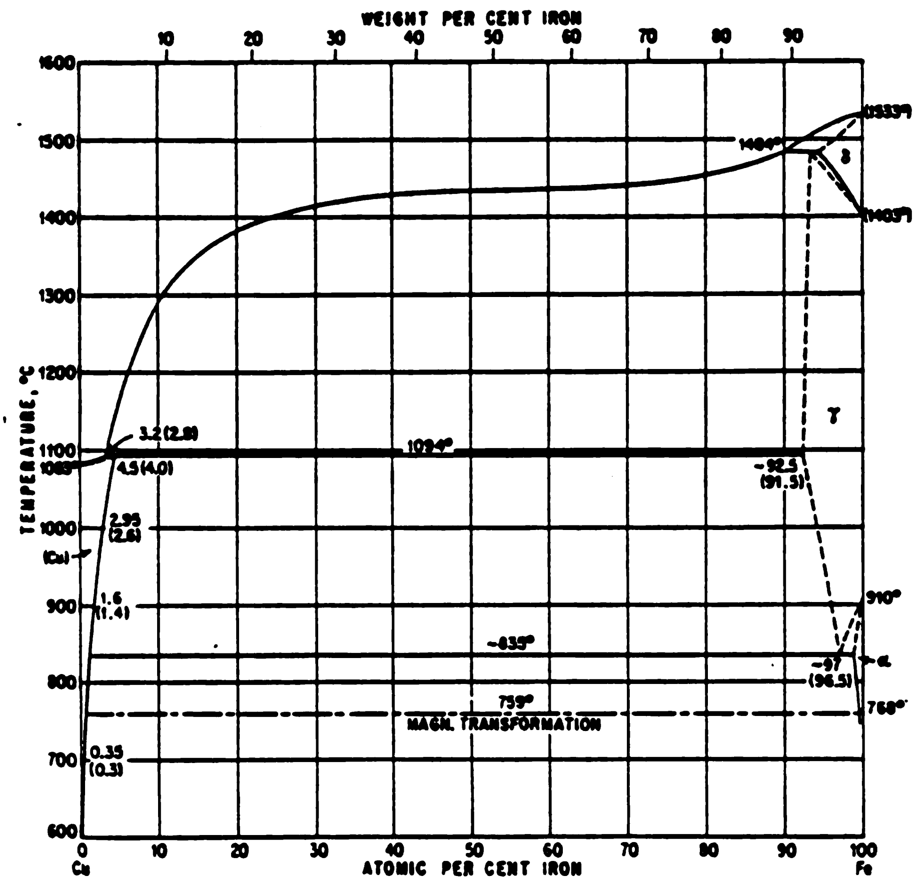

Figure 1 Equilibrium Phase Diagram of Cu-Fe

particles were found to be the f.c.c. γ-iron[3]. The size (200 Å to 3000 Å in diameter) of the γ-iron particles becomes larger as the aging time increases. According to Newkirk[3], it was only after extremely prolonged aging (4 months) that the X-ray diffraction indicated the existance of the α-iron particles. Thus, Newkirk concluded that the usual aging treatment can only produce the precipitation of the metastable γ-iron pariicles.

The coherent γ-iron particles, so formed, can stay metastable even down to the liquid helium temperature. This stabilization phenomenon of the γ-iron is now believed to be due to the strong constraint of the f.c.c. copper matrix. Easterling and Miekkoja[4] estimated the lattice parameter of the γ-iron at room temperature (3.56 Å) being only slightly smaller than the lattice parameter of copper (3.61 Å). Electron microscopy work revealed that the coherent γ-iron particles are dislocation free.

If external stress is applied to plastically deform the specimen, $\gamma \rightarrow \alpha$ transformation occurs in a martensitic manner. It was found that the transformed particles have a banded structure. These bands represent three dimensional discs which traverse the precipitate and they were initially thought as the alternative layers of transformed α-iron and untransformed γ-iron by Easterling and Miekkoja[4]. But later, it was shown by Kinsman et al.[5] that, these bands were made of twin related α-iron martensite. The banded structure of α-iron in most particles, after uniaxial deformation, was found to be aligned along the same direction. This shows the effect of applied stress on the preferential formation of specific martensite variants as studied by Kato et al.[6]. According to their analysis, the formation of the specific variants can be understood if we consider that the applied stress helps to activate the {111} <112>$_{fcc}$ shear systems necessary to change the lattice (Bain strain). Very recently, Monzen et al.[7] re-confirmed the analysis by Kato et al.[6] suggesting the role of a glide dislocation as an amplifier of the applied stress.

Corollary to the structural deformation, change in magnetic properties in the Cu-Fe system has been an interesting topic in physics. It was found that the γ-iron particles showed antiferromagnetism at low temperatures, the Néel temperature of which exists at around 67 K[8]. Although the size dependence of the Néel temperature and the possible domain structure have been suggested by solid state physisists, their analsis are not fully reliable because of the lack of intensive structural examination.

1.2 Rationale of the Present Research

Although numbers of studies have been carried out on the Cu-Fe system as shown in the previous section, we would like to list here the problems still remain to be solved which are directly related to the present research.

i) The mechanism of the $\gamma \rightarrow \alpha$ martensitic transformation

It is still not clear how the $\gamma \rightarrow \alpha$ transformation is initiated. If a dislocation plays an important role, as Monzen et al[7] suggested, what is the exact interaction between the dislocation and a particle.

ii) Morphology of the α-iron particles

The twinned structure in the deformation-induced α-iron particles should have a relationship to the plastic deformation and transformation. For example, if dislocations cut through the particles during plastic deformation, how is the twinning plane related to the slip plane of the copper matrix.

iii) Magnetic properties

Although we know that the α-iron is ferromagnetic and the γ-iron in the Cu-Fe system shows para to antiferromagnetic transformation, the examination of structure-property relationship associated with the magnetic changes is still in its infancy.

Unfortunately, these problems are too big to answer completely in the present research. However, as will be shown later we believe that we could at least cast a light on some of the related questions belonging to the above fundamental problems.

2 EXPERIMENTAL PROCEDURE

Single crystals of a Cu-1.06wt%Fe alloy were grown by the usual Bridgman method. The orientations of the single crystals were determined by the back-reflection Laue technique. Tensile specimens, 1x3x20mm, which were cut by a diamond cutter or a spark cutter from the as-grown single crystals, had their tensile directions close to the [100] direction. These were then solution-treated at 1223 K in vacuum for 6 hrs and water quenched. After the solution treatment, the specimens were aged at 973 K in vacuum for 3 hrs to 7 days and at 873 K for 12 hrs to 10 days in order to obtain γ-iron particles with about 150 - 1400 Å in diameter. A specially designed vertical furnace was constructed for these heat treatments. The furnace is capable for heating and quenching samples under vacuum and inert gas atmosphere as schematically shown in Figure 2. Following the heat treatment, the specimens were chemically polished in 50% phosphoric acid, 25% nitric acid and 25% acetic acid solution. Some of these specimens were kept for magnetic measurements and the rest were deformed 10% in tension on an Instron type testing machine with a strain rate of 1.67×10^{-3} sec^{-1} at room temperature to induce the $\gamma \rightarrow \alpha$ martensitic transformation in the small iron particles. For electron microscopic observations, these 1mm thick deformed specimens were first thinned to 0.2mm by mechanical polishing using a 240 grid paper. Then, they were thinned further to 0.1mm chemically by using a 50% phoshoric acid, 25% nitric acid and 25% acetic acid solution. After cutting discs from the 0.1mm thick

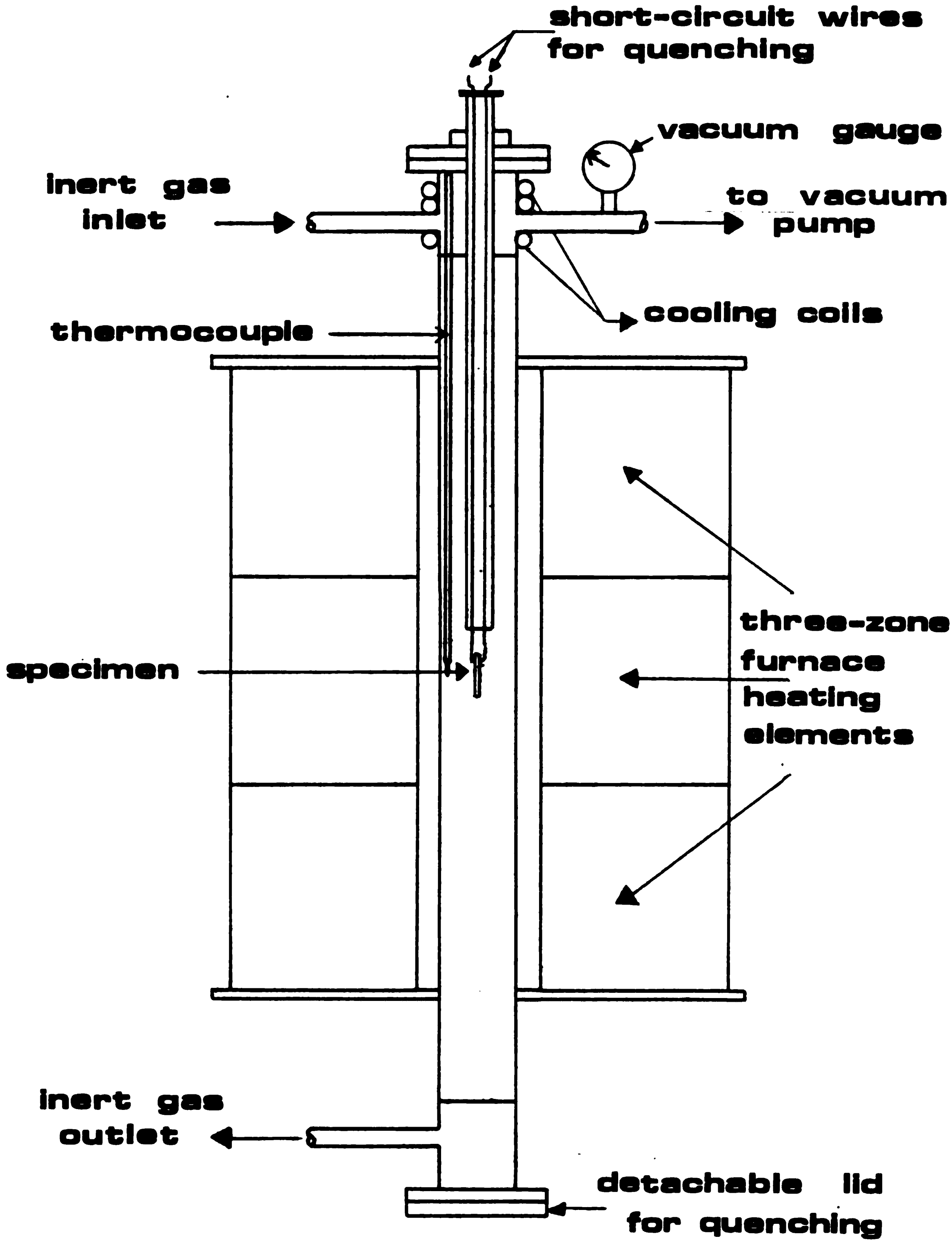

Figure 2 Schematic drawing of the furnace

specimens, they were jet polished in a 50% phosphoric acid and 50% water solution at room temperature. Final electro-polishing was accomplished with the same electrolyte at room temperature. The specimens were examined in a HU-11A electron microscope under an acceleration voltage of 100 KV.

In order to conduct the magnetic measurements, the solution treated and aged single crystals were deformed various amounts starting from the elastic region up to fracture. After spark cutting the heavily deformed grip regions, the susceptibility of these variously deformed specimens were measured by using a superconducting SQUID susceptometer under an applied magnetic field of 9750 Gauss.

3 EXPERIMENTAL RESULTS

3.1 TEM Observations

Figure 3 shows the typical appearence of the γ-iron particles formed after aging treatment for 1 day at 873 K. From the characteristic "coffee-bean" strain contrast around the particles, it is clear that the metastable γ-iron particles are coherent with the copper matrix. The lack of dislocation contrast indicates that the particles are dislocation free in agreement with the previous studies[4]. The longer aging treatment only changed the size of the particles and no α-iron particles are observed, except for the extracted ones

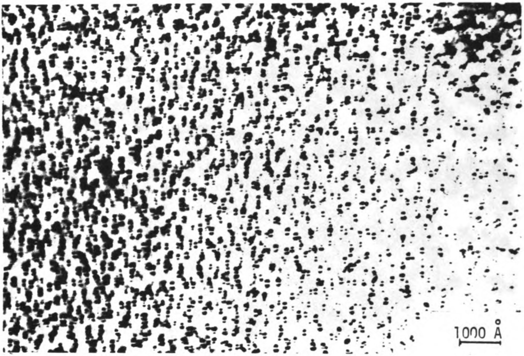

Figure 3 Micrograph showing the coherent γ-iron particles before deformation

during the thinning procedure, even in a specimen aged for 7 days at 973 K. From this, it can be concluded that aging of the Cu-1.06wt%Fe alloy for as long as 7 days at 973 K does not induce the spontaneous $\gamma \rightarrow \alpha$ phase transformation and all the iron particles in the copper matrix are in the form of the metastable γ-iron. This TEM observation was also confirmed by a magnetic test; none of the aged (but not deformed) specimens show magnetic response by the application of a magnetic field, indicating the absence of ferromagnetic α-iron.

Figure 4 shows the microstructure of the 7 day aged specimen after the room temperature deformation as much as 10%. As expected, the strain field contrast disappeared and, instead, the image of each

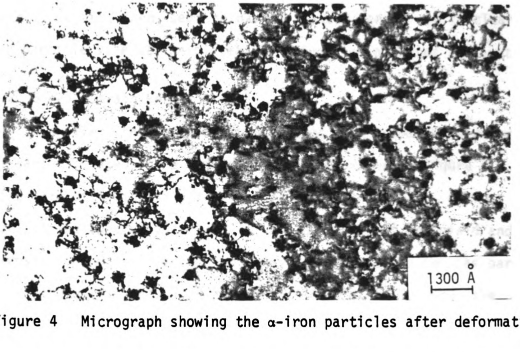

Figure 4 Micrograph showing the α-iron particles after deformation

particle can be seen as a black circle of approximately 400 Å in diameter. From this, it is concluded that the particles are in the α-form and the $\gamma \rightarrow \alpha$ martensitic transformation took place during the deformation. It can be seen from Figure 4 that the dislocations are tangled around the particles. Some of the dislocations are interconnected each other between the particles. The discussion related to this observation will be carried out later. Since the γ-iron is ferromagnetic, the $\gamma \rightarrow \alpha$ transformation can easily be detected by a magnetic measurement, the details of which will be shown in section 3.3.

Similar TEM observations were made for specimens aged from 3 hrs to 7 days at 973 K and for specimens aged from 12 hrs to 10 days at 873 K to examine the effect of aging time and temperature on the precipitation reaction of the iron particles. The observed average particle size is plotted against the aging time in Figure 5. Regardless of the aging temperature, the particle size initially increases with aging time and, then, seem to have a plateau range. It is clear that the particle size at the plateau is a function of aging temperature.

3.2 Stress-Strain Behavior

Tensile stress-strain curves during room temperature deformation of variously aged Cu-Fe single crystals are shown in Figure 6. The direction of the tensile axis was close to the $[100]_{fcc}$ and was the same for all the apecimens tested. It can be seen that the yield and flow stresses become smaller as the aging time becomes longer (as particle size becomes larger). For comparison, Figure 6 also shows the stress-strain curves of as quenched (solution treated) Cu-Fe and

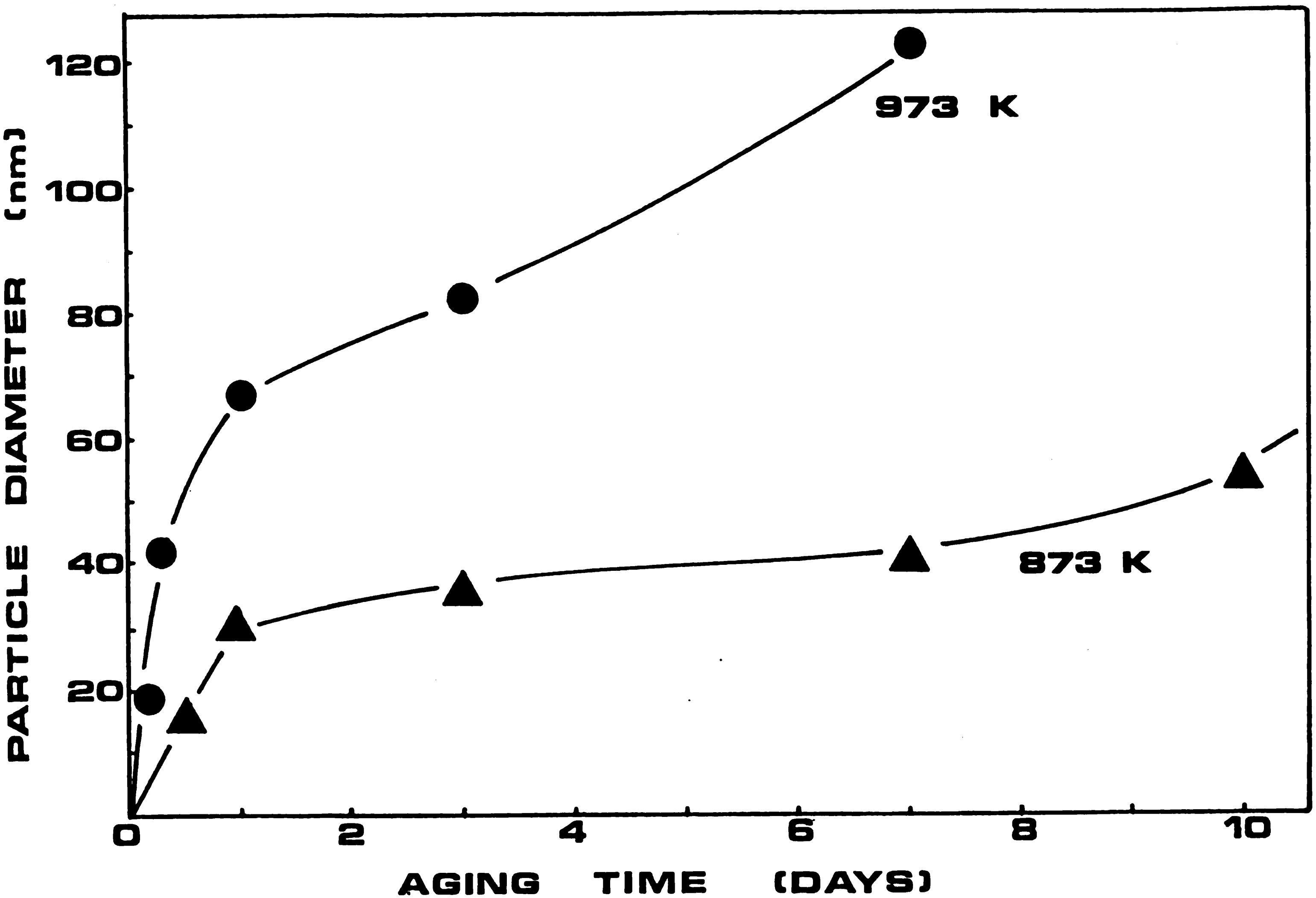

Figure 5 The average iron particle size in Cu-1.06wt%Fe alloy

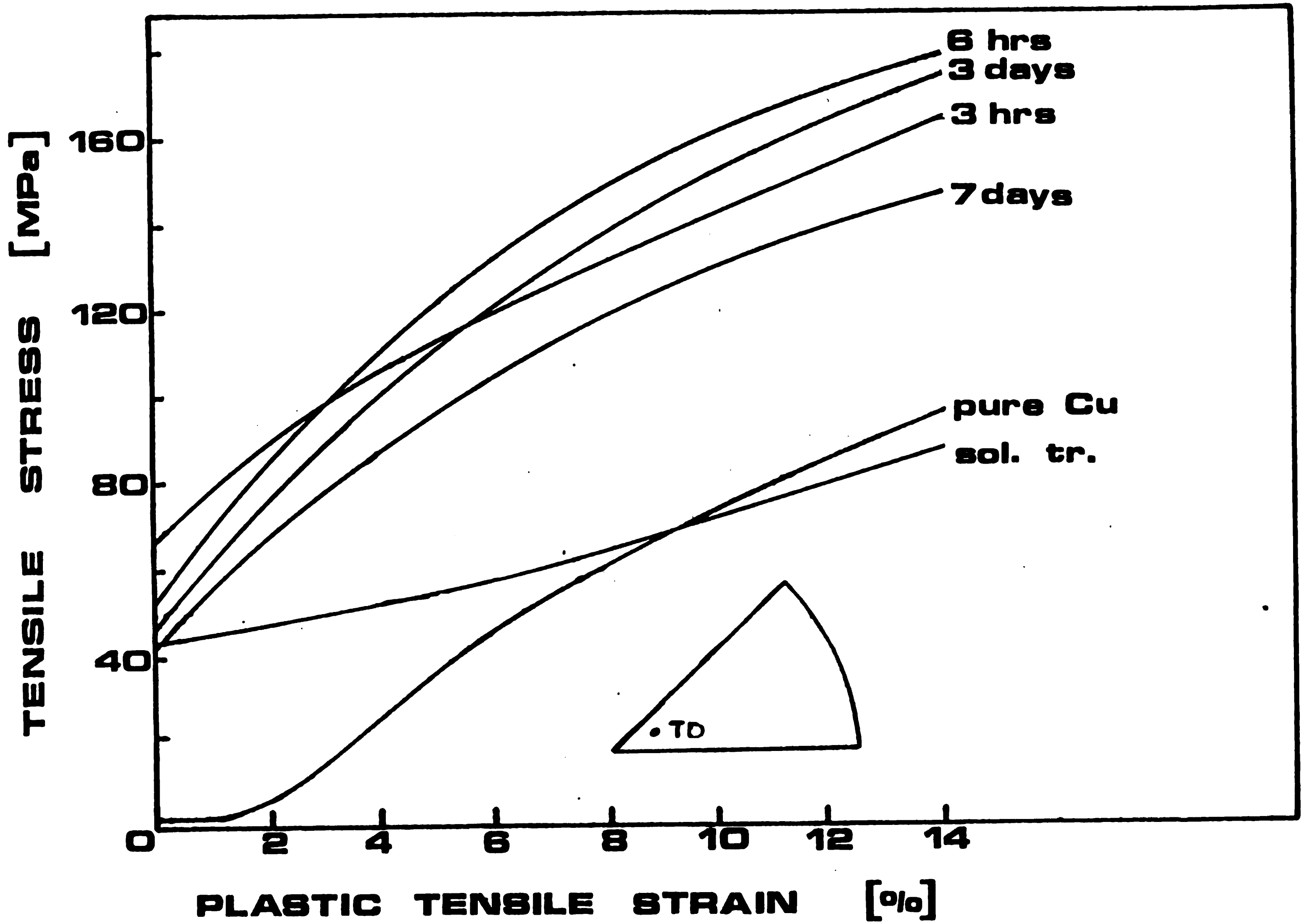

Figure 6 The stress-strain curves of Cu-1.06wt%Fe alloy aged at 973 K and pure copper

pure copper[9] single crystals deformed approximately along the same direction. It is clear that the age hardening is taking place in Cu-Fe alloy, the mechanism of which will be discussed later.

3.3 Magnetic Properties

In order to study the amount of $\gamma \rightarrow \alpha$ deformation-induced transformation, the magnetic susceptibility of the aged and deformed Cu-Fe specimens was measured by using the SQUID, Superconducting Quantum Interference Device. The applied magnetic field was 9750 Gauss and the examination was conducted at 250 K. It should be reminded that the change in the magnetic susceptibility is attributed to the para(γ) to ferro(α) magnetic transition and thus, directly related to the martensitic transformation.

The results of the susceptibility measurements are shown in Figure 7. The increase of the susceptibility readings up to a saturation point, as the plastic strain increases, is the most striking feature of the susceptibility-strain curve. This increase is more rapid in the specimens with larger iron particles. However, in the specimens with relatively smaller iron particles, for example, 6 hrs aged sample with 400 Å particle size, there exists a critical plastic strain below which the transformation is negligible.

The effect of applied stress on the martensitic transformation in the γ-iron particles was also studied by measuring the susceptibility of the Cu-Fe specimens after the deformation within macroscopically elastic range. Neither the 7 days nor the 3 hrs aged specimen showed a trace of transformation.

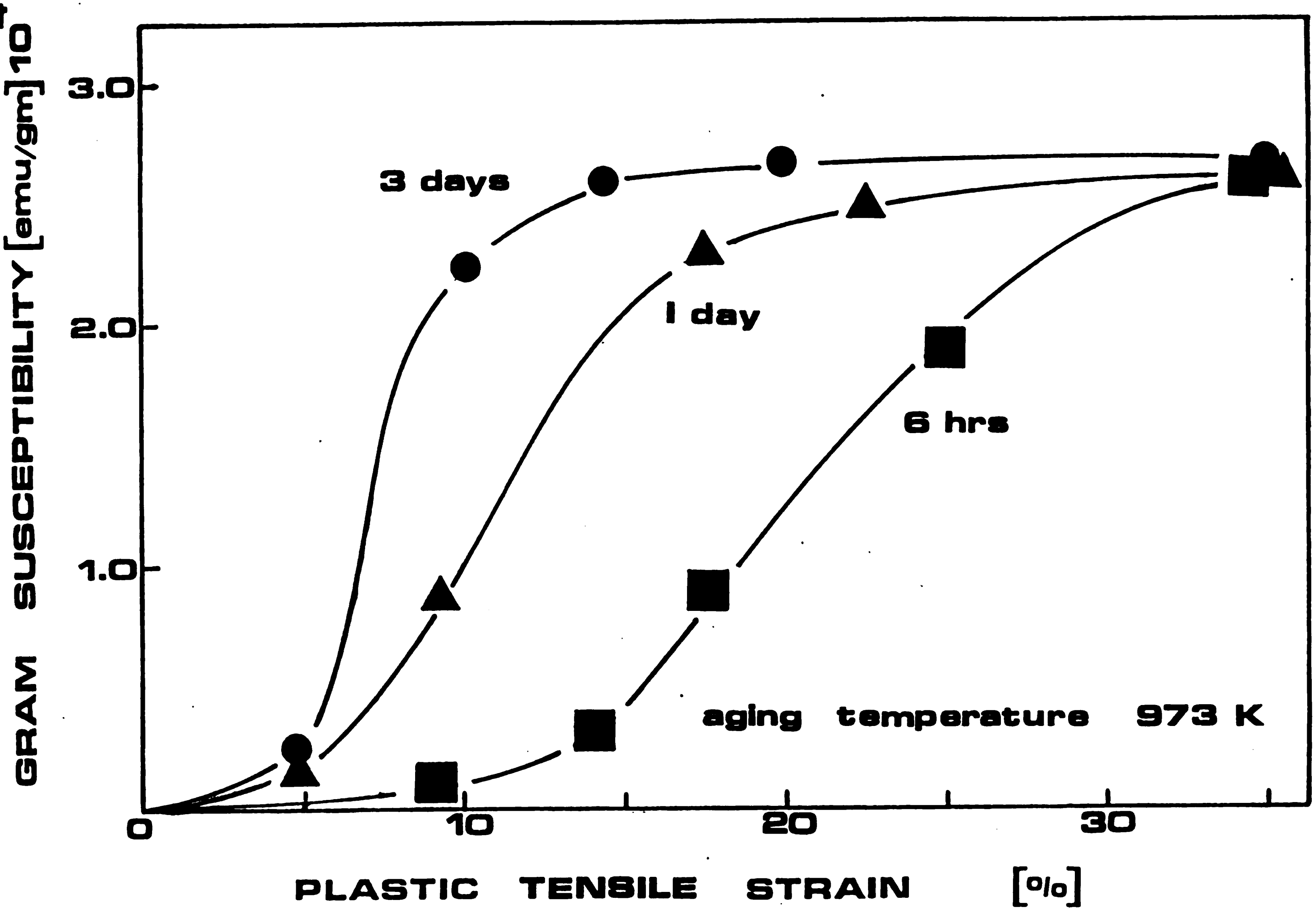

Figure 7 The change of susceptibility by deformation in Cu-Fe alloy

The above experimental observation indicates an important result that the plastic deformation is necessary before the $\gamma \rightarrow \alpha$ martensitic transformation can take place. This point will be discussed later.

4 DISCUSSION

4.1 Deformation Characteristics of the Cu-Fe Alloy

As shown in Figure 6, the aged Cu-Fe specimens with the iron particles in the copper matrix have larger yield and flow stresses than those in the pure copper. This age-hardening phenomenon is, of course, due to the creation of finely dispersed iron particles in the copper matrix and these particles act as obstacles against the motion of glide dislocations.

In order to show more clearly the effect of aging on the strength of the Cu-Fe alloy, the measured critical resolved shear stress (CRSS) is plotted against aging time in Figure 8. The CRSS is obtained from the tensile yield stress and the Schmid factor of 0.4082. It can be seen that the aging initially hardens the alloy and then softens. This is the characteristic behavior of precipitation-hardened materials.

Many investigators have studied the mechanism of the age-hardening phenomena in precipitation-hardened materials[10,11,12,13]. Although details of the theories are different, it is generally believed that when coherent particles are small, glide dislocations can cut through the particles. This process requires the additional energy (and thus stress) resulting in the hardening of the materials. When the particles become larger as the aging time becomes longer, the dislocations can no more cut through the particles and instead, they find ways of moving around the particles (the Orowan Mechanism). The critical radius of the particles r_c where the Orowan mechanism becomes operable is roughly

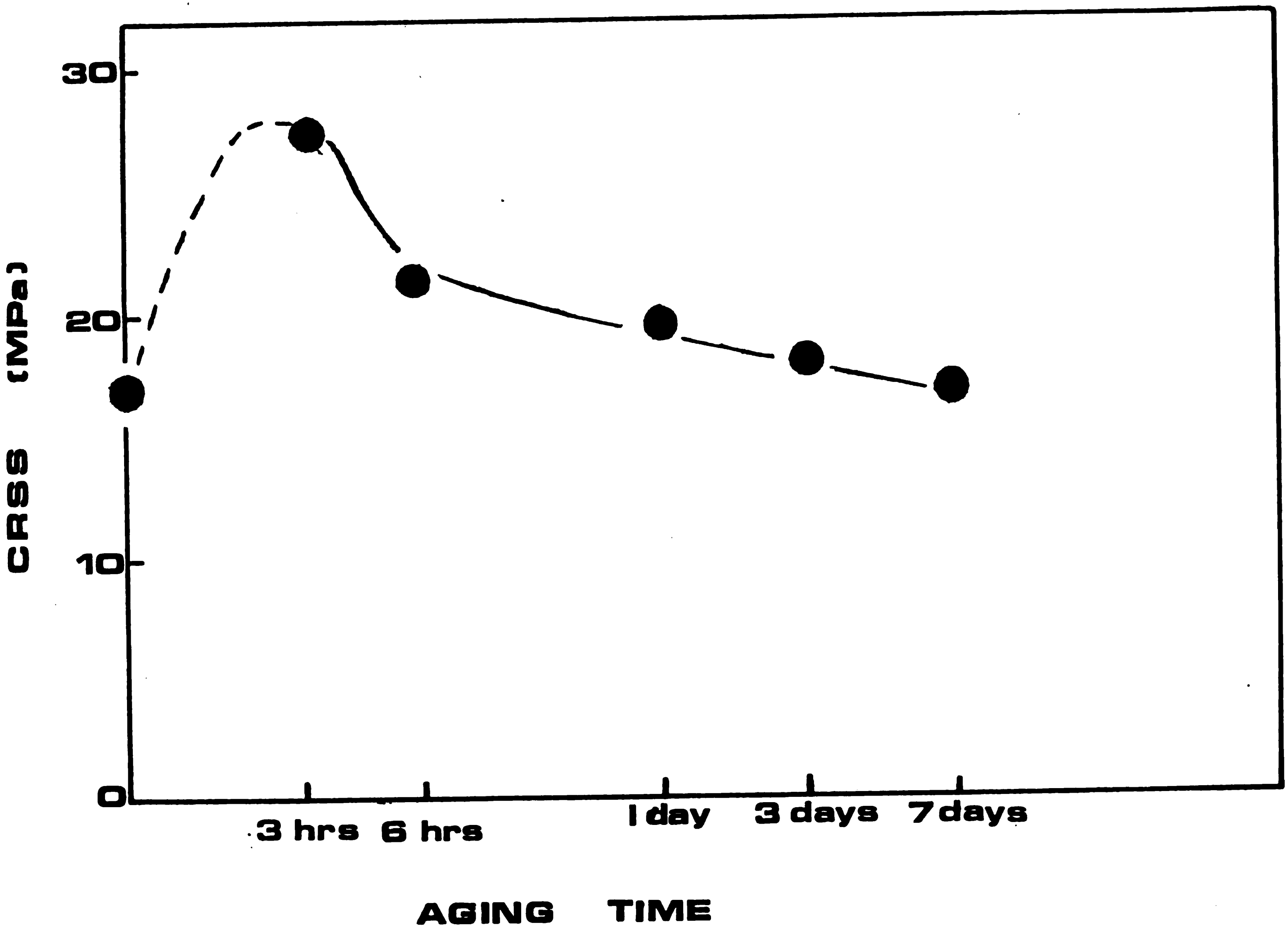

Figure 8 The critical resolved shear stress (CRSS) values of variously aged Cu-Fe specimens.

estimated as[11,12]

$$r_c \simeq \frac{2b}{3|\varepsilon|} \qquad (1)$$

where b is the magnitude of the burgers vector of a dislocation in a matrix and ε is the misfit coherency strain between the precipitate and the matrix. For the case of Cu-Fe, b=2.56 Å. The reported misfit strain ranges from -0.008[13] to -0.0125[4]. Thus for simplicity, we will assign ε=-0.01. Substitution of these values into equation (1) gives $r_c \simeq 170$ Å. This means that it is not unrealistic to assume that the dislocation cutting takes place for the 3 hrs aged specimen with average particle radius r = 95 Å (see Figure 5) and the Orowan mechanism is operative for the specimens aged longer than 6 hrs (r > 170 Å).

Keeping this in mind, in order to quantitavely discuss the experimental values of the CRSS, let us first apply the theory of the dislocation cutting by Gerold and Haberkorn[12] for the 3 hrs aged specimen. According to their study, the CRSS τ for a screw dislocation can be written as

$$\tau = G|\varepsilon|^{3/2}\left(\frac{rf}{b}\right)^{1/2} \qquad (2)$$

where G is the shear modulus of the matrix, 4.55×10^{10} Pa for copper. f is the volume fraction of the particles and can be calculated by applying the lever rule to the equilibrium phase diagram. For the 973 K aging of the Cu-1.06wt%Fe alloy, we have f = 0.0095. Substituting the values of other constants for the 3 hrs aged specimen into equation (2), we have τ = 27 MPa in good agreement with the experimental observation. Although it is true that Gerold and Haberkorn[12] predict three times larger stress than equation(2) for an edge dislocation, we think that the order of magnitude of the observed CRSS is still explained by their theory.

For alloys with larger particle sizes, the Orowan equation for the CRSS

$$\tau = \frac{Gb}{\bar{\lambda}} \tag{3}$$

will be applied. Here $\bar{\lambda}$ is the effective planer interparticle spacing and obtained from the standard formula[11]

$$\bar{\lambda} = \left(\frac{1.77}{f^{1/2}} - 2 \right) r \tag{4}$$

Equations (3) and (4) are used to obtain the theoretical CRSS for specimens aged longer than 6 hrs and the calculated results together with the experimental values are summarized in Table 1. As can be seen, the theoretical CRSS's are in good agreement with experimentally measured ones.

Woolhouse[13] also considered the effect of modulus hardening proposed by Russel and Brown[10]. We did not take this theory into account because the theory is developed for the case of softer precipitates in a harder matrix and, thus, it is still questionable whether we can simply apply their result to the Cu-Fe alloy where the harder iron particles are dispersed in the softer copper matrix.

Table 1 The measured and theoretical critical resolved shear stress values (CRSS) of Cu-Fe specimens

Aging Time at 973 K	Measured Particle Radius(A)	Effective Planer Interparticle Spacing $\lambda(10^3A)$	Theoretical CRSS (MPa)	Measured CRSS (MPa)
3 hrs	95	1.54	27 (1)	27.9
6 hrs	210	3.39	34 (2)	20.7
1 dav	335	5.41	22 (2)	19.8
3 davs	410	6.63	18 (2)	18.9
7 davs	630	10.2	11 (2)	17.1

(1) Theory of Gerold and Haberkorn

(2) Orowan Mechanism

It should be noted that here the theoretical CRSS given by equation (2) or (3) actually explains the incremental value over the CRSS of the copper matrix. However, as shown in Figure 8, The CRSS of pure copper is negligibly small compared with that of the Cu-Fe alloy. Thus, the friction stress of the copper matrix, if any, can be neglected to discuss the age hardening phenomenon.

Another noteworthy result in Figure 6 is the work-hardening rates. The initial work-hardening rate of the aged specimen is ~1.4×10^3 MPa whereas that of the solution treated (as quenched) one is ~1.8×10^2 MPa. This means that not only the dislocation motion is more difficult in aged specimens but also more obstacles such as Orowan loops and other dislocation tangles, are formed in the aged specimens than in the solution treated one during plastic deformation. Moreover, the stress strain curve of 3 hrs aged specimen crosses the stress-strain curves of longer aged specimens with a relatively low initial work-hardening rate. This verifies that in 3hrs aged specimen, the iron particles are cut by the dislocations during plastic deformation without leaving many obstacles around the particles.

The work hardening rate in the order of 1.4×10^3 MPa is commonly observed in dispersion-hardened copper base alloys with non-deformable particles[13]. However, the application of the quantitative discussion based on the Tanaka and Mori's theory[13] is not simple for the present specimens because of the possible occurence of multiple slip, due to the symmetric tensile direction close to [100], which also causes the work-hardening.

4.2 Magnetic and Structural Phase Transformations in Iron Particles

As was mentioned in section 3.3 and shown in Figure 7, the susceptibility reading by using a SQUID susceptometer is a function of both aging time and the amount of deformation. Since the γ-iron is ferromagnetic at 250 K, the change in susceptibility can be attributed to the occurence of the deformation-induced $\gamma \rightarrow \alpha$ martensitic transformation. It can be seen from Figure 7 that the susceptibility levels off as the increase of plastic deformation and the saturation value is about 2.5×10^{-4} emu/Gauss regardless of the aging time. Since the applied magnetic field is 9750 Gauss, the total magnetization μ_T per gram of the Cu-Fe alloy becomes

$$\mu_T(\text{exper.}) = 2.5 \times 10^{-4} \times 9750 \qquad (6)$$

$$= 2.43 \text{ Gauss/gram}$$

On the other hand, since the saturation magnetization of the α-iron around 250 K at which the magnetic measurements are conducted, is $M_s = 1.71 \times 10^3$ Gauss, we can estimate the theoretical value of the magnetization by assuming for simplicity that all the iron atoms are in the particles as

$$\mu_T(\text{theo.}) = \frac{1.06 \times 10^{-2} \times M_s}{\rho_{Fe}} \qquad (7)$$

$$= \frac{1.06 \times 10^{-2} \times 1.71 \times 10^3}{7.92}$$

$$= 2.29 \text{ Gauss/gram}$$

per one gram of the Cu-Fe alloy where ρ_{Fe} is the density of α-iron. Since the experimental value (equation(6)) is in good agreement with the theoretical one (equation(7)), we can reasonably say that the saturation in the susceptibility in Figure 7 occurs when all the particles are transformed into α-iron martensite.

From the above discussion and Figure 7, it can also be said that the larger the particle size, the more rapidly the deformation-induced transformation takes place. This is in qualitative agreement with the work done by Monzen et al.[7]. As it is proposed by them, the $\gamma \rightarrow \alpha$ transformation depends on the probability of the collision of a glide dislocation with an iron particle. That is, the glide dislation behaves like an amplifier of the applied stress to cause the martensitic transformation.

The question still remains why the hydrostatic tensile stress inside a γ-iron particle due to its coherency with the copper matrix is not enough to trigger the martensitic transformation, since $\gamma \rightarrow \alpha$ transformation accompanies the volume increase[15]. To examine this question, let us estimate the magnitude of the hydrostatic stress field in the γ-iron particle. From the Eshelby's theory[16,17], the stress field σ_{ij} in the spherical inclusion with the elastic constants $C^{*}_{ijk\ell}$ different from those of the matrix $C_{ijk\ell}$ can be written as

$$\sigma_{ij} = C_{ijk\ell}(S_{k\ell mn}\varepsilon^{**}_{mn} - \varepsilon^{**}_{k\ell})$$

$$= C^{*}_{ijk\ell}(S_{k\ell mn}\varepsilon^{**}_{mn} - \varepsilon^{*}_{k\ell})$$

where the ε^{*}_{ij} and ε^{**}_{ij} are respectively the true and the equivalent eigenstrains in the inclusion and $S_{k\ell mn}$ is defined for a spherical inclusion of radius r in an anisotropic material[18] as

$$S_{k\ell mn} = (8\pi)^{-1}\int_{S^2} C_{ijmn}\xi_j\{\xi_\ell N_{ki}(\underset{\sim}{\xi}) + \xi_k N_{\ell i}(\underset{\sim}{\xi})\} \times D^{-1}(\underset{\sim}{\xi})dS(\underset{\sim}{\xi}) \qquad (9)$$

where $\underset{\sim}{\xi}$ is a unit vector and the integration is performed on the surface of a unit sphere S^2. $N_{ij}(\underset{\sim}{\xi})$ and $D(\underset{\sim}{\xi})$ are, respectively, the cofactor and the determinant of the matrix whose i j component is defined as $K_{ij} = C_{ipjq}\xi_p\xi_q$. In equations (8) and (9), the usual summation convention over repeated indices is assumed.

For the present Cu-Fe alloy, we can write by using the Kronecker's delta as

$$\varepsilon^*_{ij} = \varepsilon\delta_{ij} = 10^{-2}\delta_{ij} \qquad (10)$$

The elastic constants of the copper matrix are $C_{1111} = 16.84\text{x}10^{10}$ Pa, $C_{1122} = 12.14\text{x}10^{10}$ Pa and $C_{1212} = 7.54\text{x}10^{10}$ Pa. Although the elastic constants of the γ-iron at room temperature are not available, we can approximate by using those of an austenitic 18-12 stainless steel[19] as $C^*_{1111} = 19.11\text{x}10^{10}$ Pa, $C^*_{1122} = 11.78\text{x}10^{10}$ Pa and $C^*_{1212} = 13.85\text{x}10^{10}$ Pa. The hydrostatic internal stress σ_{ij} calculated from equations (8) through (10) with the above data becomes

$$\sigma_{ij} = 1.3\text{x}10^3\delta_{ij} \text{ MPa}$$

This value is extremely large when compared with the magnitude of the uniaxial tensile stress which is in the order of 10^2 MPa from Figure 6. Quantitatively, this means that the external stress is just a very tiny fraction of the internal stress. Therefore, the fact that the γ-iron particles do not transform into α-iron martensite unless external stress is applied, strongly indicates that it is not the huge hydrostatic tensile stress but the shear component of stress which is essential for triggering the $\gamma \rightarrow \alpha$ martensitic transformation and a glide dislocation acts as an amplifier of the shear stress as discussed previously.

5 CONCLUSION

The deformation-induced martensitic transformation of iron particles in a Cu-Fe alloy was studied by examining the dependence of transformation on iron particle size and applied strain.

1. The micrographs showed that the metastable γ-iron particles are coherent with the matrix and dislocation free.
2. The longer aging treatment up to 7 days only changed the particle size and did not induce the $\gamma \rightarrow \alpha$ transformation.
3. The stress-strain behavior of Cu-Fe alloy showed a decrease in yield stress with the increased particle size. This can be essentially explained by the Orowan mechanism of dislocation motion.
4. The initial work-hardening rate of the aged specimens is much larger than that of the solution treated one. This can be attributed to the creation of obstacles (Orowan loops, dislocation tangles) in the aged specimen during plastic deformation.
5. Magnetic measurements showed that the plastic deformation was necessary in order to induce the transformation.
6. The fraction of transformed α-iron particles to the total iron particles becomes larger as the particle size and amount of strain increase. Moreover, even in the specimen with 190 Å diameter particles almost all of them transform to α-iron after 35% plastic tensile strain although this transformation was much more rapid for the larger iron particles.
7. The calculation based on elasticity revealed that a very large hydrostatic stress field exists in a γ-iron particle which is not

helpfull to induce the $\gamma \rightarrow \alpha$ martensitic transformation.

8. From the observations (5), (6) and (7), it is concluded that external stress supplies shear stress fields the existence of which is essential to cause the transformation.
9. If we assume that the role of glide dislocations on the $\gamma \rightarrow \alpha$ martensitic transformation is to amplify the shear stress field, the experimental observations can be explained in a consistent manner.

REFERENCES

1. F. Bitter and A. R. Faufman, Physical Review, 56, 1044(1939).
2. C. S. Smith, Age Hardening of Metals, p.186, A.S.M.(1940).
3. J. B. Newkirk, Transections AIME, 209, 1214(1957).
4. K. E. Easterling and H. M. Miekkoja, Acta Metallurgica, 15, 1133(1967)
5. K. R. Kinsman, J. W. Sprys and R. J. Asaro, Acta Metallurgica, 23, 1431(1975).
6. M. Kato, R. Monzen and T. Mori, Acta Metallurgica, 26, 605(1978).
7. R. Monzen, A. Sato and T. Mori, Transections of the Japan Institute of Metals, 22, 65(1981).
8. U. Gonser, C. J. Meecham, A. H. Muir and H. Wiedersich, Journal of Applied Physics, 34, 2373(1963).
9. S. Karashima, "The Strength of Metals and Alloys", Japan Institute of Metals, p.68, Sendai, Japan(1968).
10. K. C. Russell and L. M. Brown, Acta Metallurgica, 20, 969(1972).
11. L. M. Brown and R. K. Ham, "Strengthening Methods in Crystals", edited by A. Kelly and R. B. Nicholson, p.12, Elsevier(1971).
12. V. Gerold and H. Haberkorn, Physica Status Solidi, 16, 675(1966).
13. G. R. Woolhouse, Philosophical Magazine, 28, 65(1973).
14. K. Tanaka and T. Mori, Acta Metallurgica, 18, 981(1970).
15. T. Mori, P. C. Cheng, M. Kato and T. Mura, Acta Metallurgica, 26, 1435(1978).
16. J. D. Eshelby, Proceedings of Royal Society (London), A241, 376(1957)
17. J. D. Eshelby, "Progress in Solid Mechanics", 2, p.89, edited by I. N. Sneddon and R. Hill, North-Holland, Amsterdam(1961).

REFERENCES

18. N. Kinoshita and T. Mura, Physica Status Solidi, (a)5, 759(1971).

19. N. Kikuchi, Journal of the Japan Institute of Metals, 35, 518(1971).